

Development of a New High Efficiency Control Method for Fuel Cell Power Generation Systems

Takuma Endoh¹, Kazutaka Itako¹

¹ Kanagawa Institute of Technology

Abstract. This paper proposes a MEPT (Maximum Efficiency Point Tracking) control system which can detect a maximum efficiency point at high speed without a hydrogen flow meter, and compare a hydrogen consumption of the MEPT control system with that of a conventional control system. As a result, the MEPT control reduced the hydrogen consumption by 14.2% compared with the conventional control, and an effectiveness of the proposed MEPT control was confirmed.

Keywords: Fuel cell, FC, Hydrogen, MEPT.

1. Introduction

Polymer Electrolyte Fuel Cell (PEFC) is fuel cells which have low operating temperatures and are easy to miniaturize. Fuel cells have been studied mainly for use in automobiles, electric tram, and trains[1]~[8]. Currently, a development of hydrogen infrastructure for fuel cells is being considered as a national initiative, and PEFCs are also attracting attention. However, due to a high cost of hydrogen, the running cost is high compared to other forms of power generation. To operate fuel cells, it is important to increase an operating efficiency and reduce the running cost.

In this paper, we propose a MEPT (Maximum Efficiency Point Tracking) control, which is a high efficiency control to reduce a hydrogen consumption of the fuel cell. The MEPT control obtains an operating point at which the output power is the maximum compared to fuel consumption, and tracks it. By repeating this operation, the fuel cell can operate at a high efficiency point and reduce the hydrogen consumption. In addition, by defining the efficiency voltage V_e , this system enables fast response without the need for a flow meter. In this paper, the maximum power control[9],[10], which is generally used to control fuel cells and a MEPT control, were used to generate electricity for one hour each with different load patterns, and the amount of hydrogen used to generate electricity was compared.

2. Fuel Cell Power Generation

Fig. 1 depicts the basic characteristic of fuel cells. The output voltage of fuel cells is V_{FC} , the output power is P_{FC} , and the output fuel ratio is ζ . Where the output fuel ratio ζ is the output power P_{FC} to the fuel consumption H and indicates the efficiency. The higher this value means that the more efficiently the fuel cell is operating. The peak point ζ_{MAX} of ζ does not necessarily coincide with the maximum power point P_{FCMAX} .

Fig. 2 depicts the system configuration for fuel cells. This system is used for maximum power control and MEPT control, which will be described later. The PEFC, DC/DC converter, super-capacitor, and electric load are connected from left to right. The digital signal processor (DSP) controls the power generation using a data of the output voltage V_{FC} and current I_{FC} of the fuel cell, the voltage V_L and current I_L of the load side obtained from a sensors.

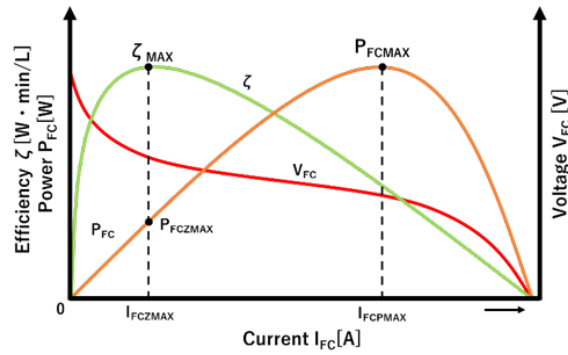


Fig. 1. Basic characteristics of fuel cells

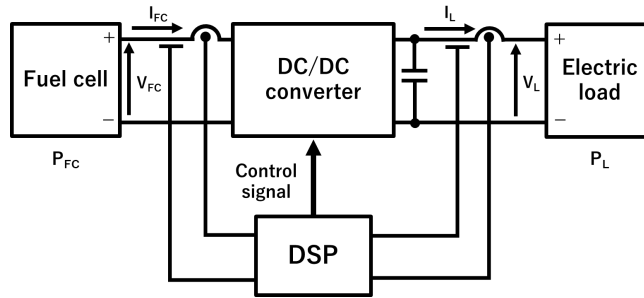


Fig. 2. Configuration of fuel cells power generation system

3. Maximum Power Control

3.1. Overview

Fig. 3 depicts operating concept of maximum power control. In the Maximum Power Control, the maximum power P_{FCMAX} is obtained by controlling I_{FC} to I_{FCPMAX} .

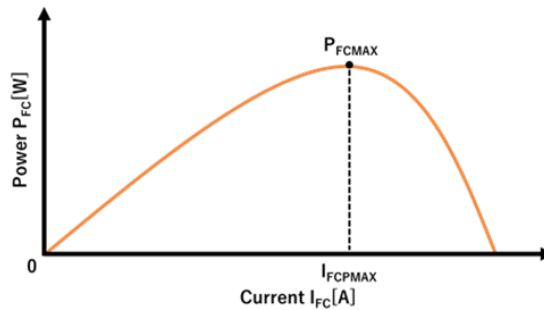


Fig. 3. Conceptual diagram of Maximum Power Control

3.2. Mode Transitions

Fig. 4 depicts the mode transition of the maximum power control. The maximum power control mode is operating at maximum power. Standby mode is executed to stop the fuel cell generation and prevent overcharging of the super-capacitor installed in front of the load. This mode lasts until the load voltage falls below a specified voltage value V_{Lmin} , and if it falls below, the maximum power control mode is executed to generate power again.

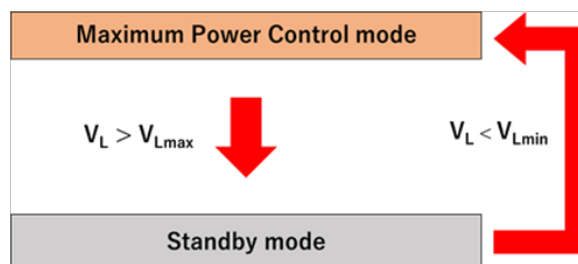


Fig. 4. Mode transitions of Maximum Power control

3.3. Problems

As shown in Figure 1, the peak point ζ_{MAX} of ζ does not necessarily coincide with the maximum power point P_{FCMAX} . Therefore, the maximum power control does not utilize the fuel efficiently, which may lead to unnecessary fuel consumption.

4. Maximum Efficiency Point Tracking Control

4.1. Overview[11],[12]

Fig. 5 depicts conceptual diagram of the MEPT control operation, which consists of three modes: ζ_{MAX} detection mode, fuel consumption suppressing mode, and maximum power control mode. ζ_{MAX} detection mode is a mode in which the operating point is gradually changed and the ζ_{MAX} is measured. The operating interval in this mode depends on the speed at which the flowmeter reaches the steady state, so it is necessary to measure and set it in advance. The fuel consumption suppressing mode is a mode to control I_{FC} to I_{FCZmax} at the detected ζ_{MAX} . In this mode, the fuel cell operates efficiently and hydrogen consumption can be suppressed. When the power at ζ_{MAX} does not reach the load power, the mode transitions to the maximum power control mode. The maximum power control mode operates at the maximum power point to compensate for a missing power. However, since this mode operates outside of ζ_{MAX} , the power generation efficiency will decrease.

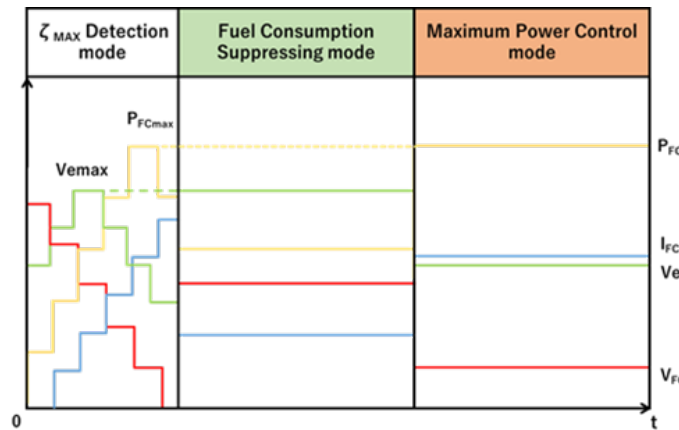


Fig. 5. Conceptual diagram of MEPT control operation

4.2. Mode Transitions

Fig.6 depicts the mode transition of MEPT control. The ζ_{MAX} detection mode detects the ζ_{MAX} . The fuel consumption suppressing mode suppresses fuel consumption by operating at the operating point of ζ_{MAX} . The maximum power control mode is a mode to operate at the maximum power point when the load power P_L exceeds the power P_{emax} at ζ_{MAX} . The standby mode operates in the same way as the maximum power control method.

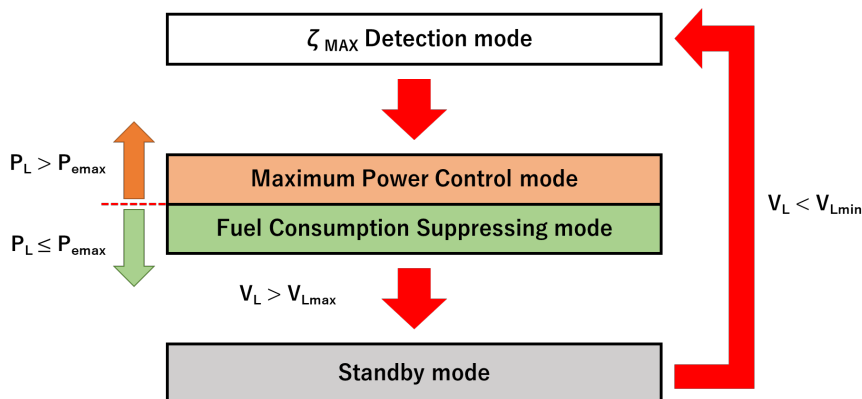


Fig. 6. Mode transitions of MEPT control

4.3. Problems

In the MEPT control, it is necessary to detect a hydrogen flow rate to obtain ζ_{MAX} . However, when a flow meter is used, it takes time to detect ζ_{MAX} because it waits for the flow meter to reach a steady state. In the meantime, there is a problem of wasted fuel. Therefore, in order to improve the response when ζ_{MAX} is detected, we define a parameter, an efficiency voltage V_e , which is similar to ζ .

4.4. Relationship between Efficiency ζ and Efficiency Voltage V_e

The output fuel ratio ζ is expressed by the following equation (1) using the fuel cell output power P_{FC} and the amount of incoming hydrogen H .

$$\zeta = \text{Output power } P_{FC} [\text{W}] / \text{Hydrogen flow rate } H [\text{L}/\text{min}] \quad (1)$$

According to Faraday's law of electrolysis, the amount of incoming hydrogen H is proportional to a sum of the fuel cell output current I_{FC} and the crossover current I_{FC0} . Therefore, it can be expressed by the following equation (2).

$$\zeta = P_{FC} / \{K(I_{FC} + I_{FC0})\} \quad [\text{W} \cdot \text{min} / \text{L}] \quad (2)$$

Where K is the proportionality constant. This equation (2) with the proportionality constant K removed is defined as the efficiency voltage V_e .

$$V_e = P_{FC} / (I_{FC} + I_{FC0}) \quad [\text{V}] \quad (3)$$

Since the efficiency voltage V_e is similar to ζ , we can obtain the same peak point as ζ . Since the efficiency voltage V_e uses the crossover current as a parameter, it is necessary to measure it beforehand. For the measurement, the amount of hydrogen used for power generation ($H-H_0$) is proportional to the output current I_{FC} , and the amount of crossover hydrogen H_0 is proportional to the crossover current I_{FC0} . Therefore, this can be calculated using the following equation (4).

$$I_{FC0} = H_0 \cdot I_{FC} / (H-H_0) \quad [\text{A}] \quad (4)$$

Fig. 7 depicts the comparison of ζ and V_e for output current I_{FC} of the PEFC used in this paper. In the FC used in this experiment, the I_{FC0} used to calculate V_e was 0.733[A] using the equation (4). As shown in the figure, ζ and V_e are similar, and V_e has a peak point at almost the same current I_{FCZmax} . From the above, it can be seen that V_e is a parameter which can replace ζ without requiring the hydrogen flow rate H .

By using this V_e for MEPT control, the flowmeter can be removed from the system, and the maximum efficiency point can be detected at high speed.

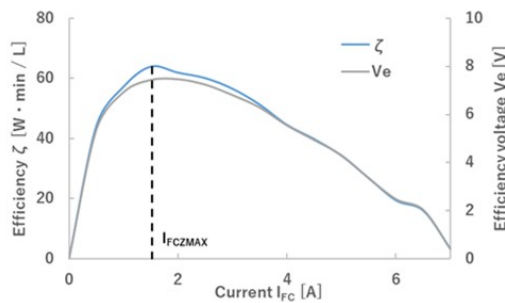


Fig. 7. Comparison of ζ and V_e

4.5. Proposed systems

Fig. 8 depicts conceptual diagram of the proposed system. The proposed system replaces the ζ_{MAX} detection mode of the MEPT control with the V_{eMAX} detection mode, which detects V_{eMAX} every time the fuel cell starts up from the standby mode by changing output voltage of the fuel cell from open circuit voltage to voltage at maximum output current of the fuel cell. The maximum output current of the fuel cell is limited because the fuel cell may deteriorate if the output current is higher than the rated value.

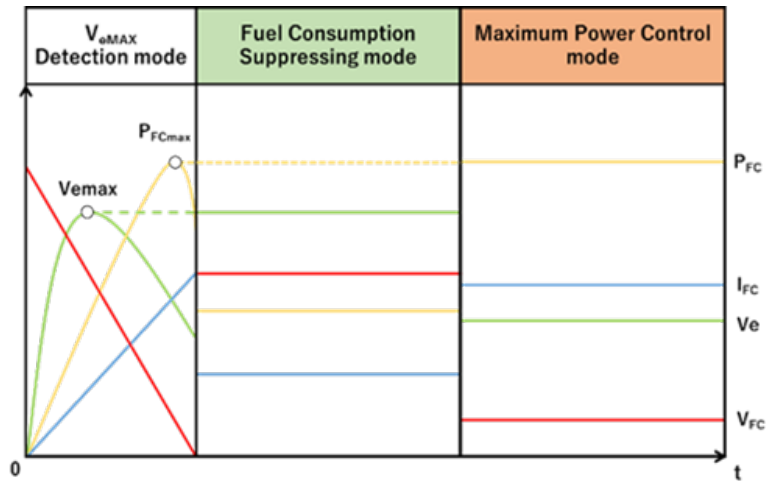


Fig. 8. Conceptual diagram of the proposed system

Fig. 9 depicts the mode transition of the proposed system. V_{eMAX} detection mode detects V_{eMAX} every time the fuel cell starts up from the standby mode, so that it can track the maximum efficiency point even when an environment changes.

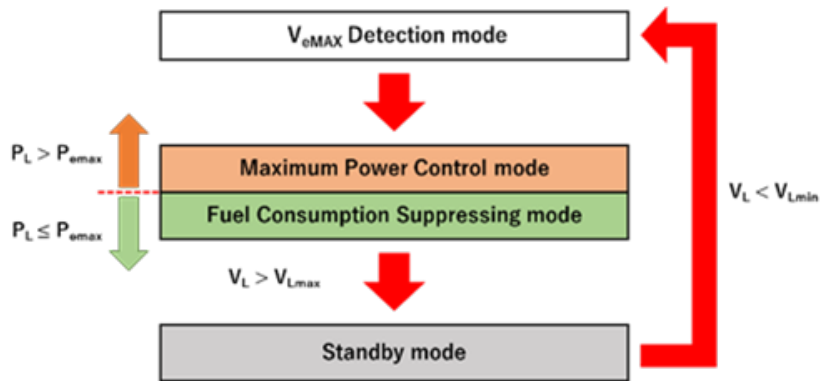


Fig. 9. Mode transition of the proposed system

5. Experiment

5.1. Outline of the Experiment

In the experiment, the system shown in Figure 2 is used to operate the fuel cell by MEPT control and maximum power control, and both hydrogen consumptions are compared. The maximum power P_{FCMAX} of the PEFC used in the experiment is 30 [W], and the operating current I_{FCMAX} is 3.5 [A]. The operating temperature of the PEFC is 27[°C]. The super-capacitor used in the experiment has a capacitance of 110[F]. The upper voltage V_{LMAX} is 24[V], and the lower voltage V_{LMIN} is 22[V].

5.2. Experimental Results

Fig. 10 depicts the load pattern used in the experiment. It shows the load pattern of an ordinary household in summer, adjusted to the 40W level and 1 hour. Using this load pattern, MEPT control and maximum power control were operated.

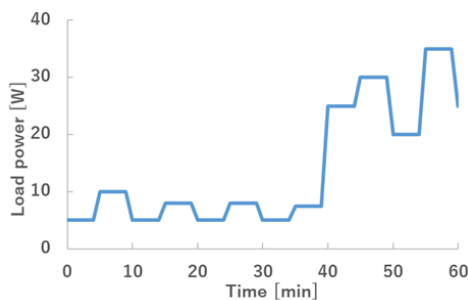


Fig. 10. Loading pattern used in the experiment

Fig. 11-(a) depicts the output voltage V_{FC} , output current I_{FC} of the fuel cell, load voltage V_L and load current I_L for maximum power control.

Fig. 11-(b) depicts the output power P_{FC} of the fuel cell and load power P_L for maximum power control. The system is operating in the maximum power control mode in region ①, standby mode in region ②. From the two diagrams, mode transitions are executed correctly and the load power P_L can be supplied according to the load pattern. The total amount of consumed hydrogen was 23.2 [L].

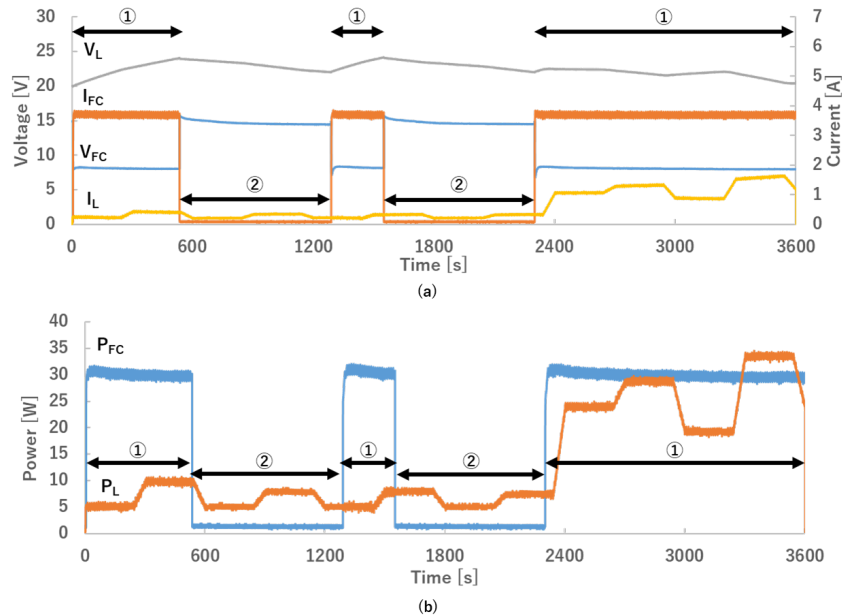


Fig. 11. Experimental results of maximum power control

Fig. 12-(a) depicts the output voltage V_{FC} , output current I_{FC} of the fuel cell, load voltage V_L and load current I_L for proposed system.

Fig. 12-(b) depicts the output power P_{FC} of the fuel cell and load power P_L of MEPT control. The system is operating in the fuel consumption suppressing mode in region ①, the maximum power control mode in region ②, and the standby mode in region ③. From the two diagrams, mode transitions are executed correctly and the load power P_L can be supplied according to the load pattern. The total amount of consumed hydrogen was 19.9[L]. Therefore, it was reduced by about 14.2% based on the hydrogen consumption of the maximum power control.

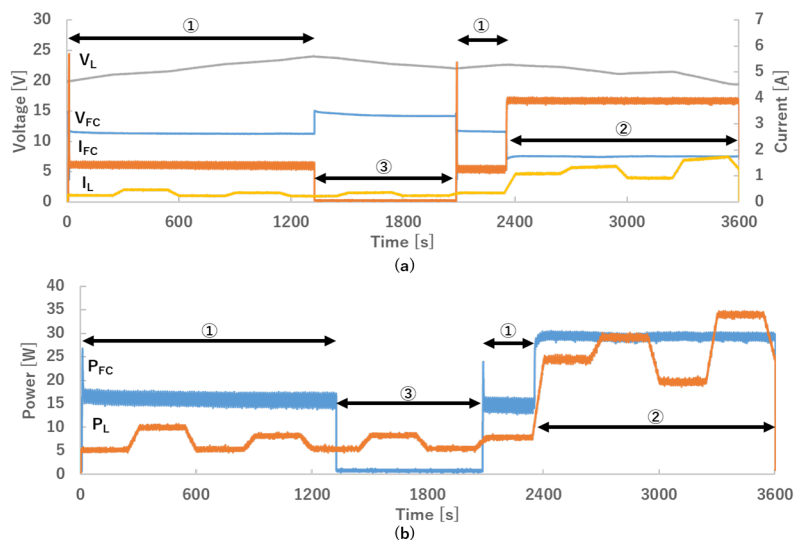


Fig. 12. Experimental results of proposed system

6. Conclusion

In this paper, we propose a fast and maximum efficiency point detectable MEPT control for fuel cell power generation systems using a newly defined efficiency voltage V_e without a hydrogen flow meter, and we compare the hydrogen consumption of the MEPT control system with that of the conventional maximum power control system. As a result, the MEPT control reduced the hydrogen consumption by 14.2% compared with the conventional maximum power control, and the effectiveness of the MEPT control was confirmed.

7. References

- [1] Wang, P., Bi, H. & Che, Y. (2019) "A Capacitor Clamped H-Type Boost DC-DC Converter with Wide Voltage-Gain Range for Fuel Cell Vehicles," in IEEE Transactions on Vehicular Technology, vol. 68, no. 1, pp. 276-290, Jan. 2019. doi: 10.1109/TVT.2018.2884890
- [2] Yan, Y., Li, Q., Chen, W., Su, B., Liu, J. and Ma, L. (2019) "Optimal Energy Management and Control in Multimode Equivalent Energy Consumption of Fuel Cell/Super capacitor of Hybrid Electric Tram," in IEEE Transactions on Industrial Electronics, vol. 66, no. 8, pp. 6065-6076, Aug. 2019. doi: 10.1109/TIE.2018.2871792
- [3] Abbas, M., Cho, I. & Kim, J.(2018) "Investigation and Control of Fuel Cell dynamics in Fuel-Cell Hybrid Railway Propulsion System,"2018 International Conference on Power Generation Systems and Renewable Energy Technologies (PGSRET), Islamabad, Pakistan, pp. 1-6. doi: 10.1109/PGSRET.2018.8686002
- [4] P. V. Gokila, K. Prithivi and L. A. Kumar, "Design and control of power conditioning unit for fuel cell hybrid vehicle," 2017 International Conference on Innovations in Information, Embedded and Communication Systems (ICIIECS), 2017, pp. 1-8, doi: 10.1109/ICIIECS.2017.8276037.
- [5] M. Neuburger and D. J. Thrimawithana, "A new topology for fuel cell power trains including a new integrated converter," 2015 IEEE 13th Brazilian Power Electronics Conference and 1st Southern Power Electronics Conference (COBEP/SPEC), 2015, pp. 1-4, doi: 10.1109/COBEP.2015.7420097.
- [6] S. Sreemathy and M. Karthik, "Modeling and performance analysis of neural network based fuel cell driven electric traction system," 2015 International Conference on Innovations in Information, Embedded and Communication Systems (ICIIECS), 2015, pp. 1-6, doi: 10.1109/ICIIECS.2015.7192991.
- [7] M. Sagar Bhaskar et al., "Survey of DC-DC Non-Isolated Topologies for Unidirectional Power Flow in Fuel Cell Vehicles," in IEEE Access, vol. 8, pp. 178130-178166, 2020, doi: 10.1109/ACCESS.2020.3027041.
- [8] W. Andari, M. S. BEN YAHIA, H. Allagui and A. Mami, "Modeling and Simulation of PEM Fuel Cell/Supercapacitor hybrid power sources for an electric vehicle," 2019 10th International Renewable Energy Congress (IREC), 2019, pp. 1-6, doi: 10.1109/IREC.2019.8754584.
- [9] K.Kobayashi and H.Fujimoto, Japan Patent 2008-10220 A (2008).
- [10] M.Takada and K.Takatsu, Japan Patent 2005-63901A(2005).
- [11] K.Itako and Sumon Md Shariful Islam "Improvement of output efficiency of a fuel cell by using Oxygen" International Journal of Technology and Engineering studies, Vol.5, No.2, pp.47~54, 2019
- [12] K.Itako, T.Suzuki, S.Daidouji and T.Mori, the 78th Meeting the Electrochemical Society, Japan, No.PFC30 (2011).